

Fuel Cells for Shipping. An Approach towards Dynamic Safety Assessment

Tomaso Vairo*, Davide Cademartori, Maria P. Carpanese, Davide Clematis, Antonio Barbucci, Bruno Fabiano

DICCA – Civil, Chemical and Environmental Engineering Department - University of Genoa, Via Opera Pia, 15 – 16145 Genoa, Italy
tomaso.vairo@edu.unige.it

Progressing limits on pollutant emissions force ship owners to reduce the environmental impact of their operations. Fuel cells may provide a suitable solution especially when compared with emissions from diesel engines in line with a more sustainable development in the shipping industry. This work deals with the safety issues related to the use of Fuel Cells in maritime application. A method for identifying and intercepting critical events, focusing on the early detection of the systems weak signals, and thus enhancing the resilience of the whole system, is designed, and applied to a Solid Oxide Fuel Cell (SOFC) system. The system relies on the abductive Bayesian inferential approach and it has been built as a Hidden Markov Model (HMM) using the Baum–Welch algorithm, which is a special case of the Expectation Maximization (EM) algorithm used to find the unknown parameters of the HMM. The proposed method integrates classical process parameters, such as temperature, flow, pressure, with on time electrochemical measurements. The proposed HMM can predict with a remarkable accuracy the most probable sequence of the systems safety state.

1. Introduction

Within the current challenge towards energy transition and connected need low-carbon fuels replacing conventional fuels and thereby minimizing life cycle emissions, transport is recognized as one of the key applicative field of application for hydrogen. Namely, hydrogen produced from fossil resources with CO₂ capture, hydrogen by electrolysis with low-carbon power and hydrogen by biogas reforming, or biomass gasification are among the options considered for this shift in transportation fuels. Different techniques along, or downstream the process were developed to decrease CO₂ emissions, such as energy efficiency improvement, by substituting less carbon-intensive fuels, or reutilization of unwanted by-products, i.e. hydrogen sulphide and carbon dioxide and obtain syngas by new technologies (Vianello et al., 2022). Additionally, energy diversification, when based on renewables, can eliminate emissions and green hydrogen produced by a bioreactor was considered for the design of phosphoric acid fuel cell of a target power (Palazzi et al., 2002), but the true potential and viability seem requiring further investigation for non-stationary applications. Electrical power in ships is mainly used for auxiliaries, although there is a tendency towards the use of electricity for propulsion as well. A vast majority of ships currently uses diesel generators to produce electricity, where chemical energy is converted into electricity via thermal and mechanical energy. Fuel cells directly convert chemical energy into electrical energy, thus omitting the indirect route via thermal energy in combustion engines. Fuel cells are modular in nature and the intrinsic performance of a single cell is not different from a large stack. As a result, power production can be distributed over the ship without a penalty of increased fuel consumption, while electricity transport losses are reduced, and redundancy is improved. For this reason, fuel cell systems are successfully applied in back-up power systems and data centres. A variety of fuel cell types with distinct characteristics has been developed over the time, e.g., low and high temperature polymer electrolyte membrane fuel cell (LT/HT-PEMFC); solid oxide fuel cell (SOFC); phosphoric acid fuel cell (PAFC) and molten carbonate fuel cell (MCFC). Among them the three most promising technologies for marine use low and high temperature PEMFC and the SOFC (Van Biert et al., 2016).

2. Materials and methods

2.1 Solid Oxide Fuel Cells

The state-of-the-art SOFCs are made by two porous electrodes (anode and cathode) which enable the migration of both electrons and ions, and one dense electrolyte where only ionic conductivity takes place. The most common anodes are composed by a cermet of Ni-YSZ, the electrolyte by YSZ and the cathode by a cermet of LSCF-GDC. SOFCs find major applications in the context of large on-shore power generation plants but, recently, they are gaining increasing interest also in the transport sector. They operate at high temperature (600-900 °C) and carry out an exothermic electrochemical reaction, which provides excess heat that can be exploited for cogeneration. SOFCs possess higher efficiency compared to other fuel cells reaching up to 85% of energy efficiency when they are coupled to gas turbines. The fuel cell is flexible towards different fuels, with the reforming from hydrocarbons to hydrogen taking place either in external reacting units sustained by the heat coming from the SOFC reaction or, even, directly inside the cell, depending on the anode electrocatalyst and plant design. A promising development for the SOFC technology is hybrid systems combining SOFC, heat recovery and batteries. This leads to the possibility of a more flexible operation of the system and, with less cycling of the SOFC, the problems associated with short cycle life are reduced. The SOFCs show higher flexibility towards fuels, compared to other fuel cell types, being able to use hydrogen, ammonia, LNG, methanol and hydrocarbons as diesel. The major emission from the SOFC is CO₂, but this is eliminated if hydrogen or ammonia are used as fuel. There are two standard geometries for SOFCs, namely planar and tubular one: even though the tubular SOFC is more stable towards thermal cycling, the planar SOFC is considered the more favourable design, due to a higher energy density and simpler design and assembling (Tronstad et al., 2017).

2.2 The predictive model

Abduction derives the best explanations for observations. Statistical abduction attempts to define a probability distribution over explanations and to evaluate them by their probabilities (Thagard et al., 1997). The framework of statistical abduction is general since many well-known probabilistic models (Galagedarage et al., 2019), i.e., Bayesian Networks (BN), Hidden Markov Models (HMMs) and Tree-based probabilistic models are formulated as statistical abduction (Sato and Kameya, 2001).

In a logical framework, abduction, is usually defined as follows:

- Given: Background knowledge B and observations O, both represented as sets of formulae in first-order logic, where O is typically restricted to a conjunction of ground literals.
- Find: A hypothesis H, also a set of logical formulae, such that $B \cup H \not\models \perp$ and $B \cup H \models O$.

Where \models means logical entailment and \perp means false, i.e., find a set of assumptions that is consistent with the background theory and explains the observations. There are generally many hypotheses H that explain a particular set of observations O. The two logical steps for the model are prediction of critical variables values and identification and location of precursors (see e.g. Vairo et al., 2021). An HMM is a generative probabilistic model, in which a sequence of observable X variables is generated by a sequence of internal hidden states Z. The hidden states are not observed directly and the transitions between hidden states are assumed to have the form of a first order Markov chain. The starting probability vector π and a transition probability matrix A are considered to specify them. The emission probability of an observable can be any distribution with parameters θ conditioned on the current hidden state. This work conceives the hidden states between a regular performance and a failure of a sub-system. The only known states are the first one (i.e., the component is performing well) and the last one (i.e., the component fails), while the hidden states in between may cautiously be considered as the precursors of accidental events. The resulting outputs of the system are the process variable values. The abductive inference in the developed HMM relies on the Metropolis Hastings (MH) sampling algorithm that performs forward and backward inference by computing the distribution space of the model parameters and determine the most likely outcome. The HMM describes the joint probability of a collection of "hidden" and observed random variables. It relies on the assumption that the i-th hidden variable given the (i - 1)-th hidden variable is independent of previous hidden variables, and the current observation variables depend only on the current hidden state. The *Baum-Welch* algorithm uses the well-known EM algorithm to find the maximum likelihood estimate of the parameters of a HMM given a set of observed feature vectors. Let X_t be a discrete hidden random variable with N possible values (i.e. N states). The $P(X_t | X_{t-1})$ is independent of time t, which leads to the definition of the time-independent stochastic transition matrix:

$$A = \{a_{ij}\} = P(X_t = j | X_{t-1} = i) \quad (1)$$

$$\text{The initial state distribution (i.e. when } t=1) \text{ is given by: } \pi_i = P(X_1 = i) \quad (2)$$

The observation variables Y_t can take one of K possible values. The probability of a certain observation y_i at time t for state $X_t = j$ is provided by: $b_j(y_i) = P(Y_t = y_i | X_t = j)$ (3)

Taking into account all the possible values of Y_t and X_t , the $N \times K$ matrix $B = \{b_j(y_i)\}$ is obtained, where b_j belongs to all the possible states and y_i belongs to all the observations. Therefore, an observation sequence is given by $Y = (Y_1 = y_1, Y_2 = y_2, \dots, Y_T = y_T)$. On these grounds, we can describe a hidden Markov chain by $\theta = (A, B, \pi)$ and by the Baum–Welch algorithm finding the HMM parameters θ that maximize the probability of the observation.

2.3 Experimental setup

Circular button solid oxide cell provided by the company SOLIDpower S.p.A were tested to retrieve electrochemical data for the predictive model. The tested cells, holding an active area of 0.28 cm^2 , are anode-supported cells, made out of a Ni-YSZ anode, a YSZ electrolyte, a GDC10 barrier layer and a LSCF-GDC10 cathode. They were investigated inside an in-house high temperature tubular test rig to measure their electrochemical performance by Electrochemical Impedance Spectroscopy (EIS). The samples were placed in between two alumina concentric tubes which act as gas flow channels. The inner tubes provide the electrodes with the respective feeding gases while the outer ones facilitate the expulsion of the exhausts. The cells were tested under the two-electrodes configuration, connecting the cathode to the working electrode and the anode to the counter. In order to ensure the gas tightness of the system and avoid fuel crossover, a sealing annulus made out of Thermiculite® 896 (Flexitallic group) and a paste of arabic gum and talc is placed on both sides of the cells. The electrical contact between the electrodes and the platinum wires inside the test rig is ensured by current collectors and platinum nets, with the latter directly attached to the end of the Pt wires inserted inside the inner tubes. The cathode current collector is LSC, which was previously screen printed over the electrode, while a Ni mesh was employed as anode current collector. The test rig setup is schematically depicted in Figure 1.

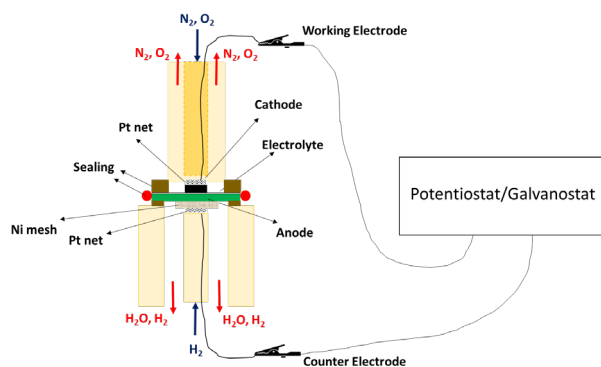


Figure 1: Test rig experimental setup.

2.4 Simplified Risk Assessment (RA)

A simplified Risk Assessment analysis was performed starting with a Failure Mode and Effects Analysis of critical components in order to identify meaningful accident scenarios. The main identified accident scenarios are as follows.

Strong exothermic reaction of reformer material

Charging the catalytic reformer material, where used, with oxygen, leads to a strong exothermic reaction. Three mechanisms leading to this process deviation were identified, namely: Loss of integrity of the fuel reformer; Reformer pressure lower than exhaust air pressure; Loss of primary fuel for fuel reforming. The recommendation is that the design of the reformer unit has to withstand fuel leaks without leading to unsafe situation.

Internal leakage in FC Module

Cracking of fuel cell plates may cause internal leakages in all three types of Fuel Cell Modules, leading to high stack temperatures and internal oxidation processes or internal fire. The stack temperature and voltage monitoring will lead to a shutdown of the corresponding stack. Two further recommended actions were identified. The amount of fuel in the fuel cell space and the corresponding consequences shall be evaluated for each configuration. Safety devices are to be designed to handle maximum credible release scenario. Combustible material in fuel cell modules shall be minimized.

Other identified accident scenarios, more related with the bunkering facility and not investigated in this paper, are: *High-energy collision penetrating LH₂ tank; Rupture of CH₂ tank containment system; Leakage of hydrogen rich gases; Failure of fuel pressure reduction; Failure of the electrical power output conditioning system; Thermal runaway of on-board energy buffer; Loss of inert gas system; Leakage during hydrogen bunkering.*

2.5 Electrochemical investigation

Working parameters are important for understanding SOFC behaviour, among which gas leakage is worth to be considered. Not only will the fuel efficiency decrease, but the gas leaked from cells may mix with oxygen outside and lead to an explosion scenario. Ideally, the electrolyte between the anode and cathode in SOFC should be completely dense with no residual porosity. However, fabrication flaws, long term degradation or other external causes may occur and lead to internal fuel crossover between the anode and cathode side, significantly reducing the performance of the cells. Special test rigs are often established for gas leakage of SOFCs. This test, however, is time-consuming and cannot give feedback during fuel testing. Rasmussen et al. (2008) introduced a method of gas leakage calculation by measuring partial pressure of anode and cathode side. The internal gas leak through the electrolyte was quantified under different conditions, as was the external leak from the surroundings of the anode. The internal gas leak did not depend on the pressure difference between the anode and the cathode gas compartment and can thus be described, as diffusion driven. External leaks between the surroundings and the anode, not involving at all the cathode gas compartment was experimentally observed. They were influenced by the pressure difference and are thus driven by both concentration and pressure gradients. EIS analysis is a powerful diagnostic technique (Lasia, 2014), adopting a frequency response analyser (FRA) to apply either a small AC voltage, or a current perturbation signal to a cell and to measure its output signal for a wide frequency range. It allows assessing the electrochemical performance of SOFCs and identify their major weak points. EIS, DRT and equivalent circuit models are often combined to quantify the impedance of the system (Jia et al., 2017, Mousa et al., 2014), finding and matching the time constants of the major resistive contributions and withdraw an electrical circuit model. Impedance spectroscopy can characterize many of the electrical properties of materials and phenomena taking place at the interfaces. In order to test the actual capability of the approach, we considered a cell under the operating conditions summarized in Table 1, which allowed obtaining experimental data utilized to train the predictive model. As already remarked, the aim is to locate and identify the conditions which may anticipate an internal leakage and predict the following cell behaviour, thus attaining a continuous evaluation and refinement of the overall system risk picture.

Table 1: Cell operating conditions

Operating conditions	
Temperature	750 °C
Fuel Channel Volumetric Flow rate	78.5 Nml/min (100% H ₂)
Air Channel Volumetric Flow rate	11.304 Nml/min (different partial pressures)
Active Area	0.2826 cm ²
Operating point	
Voltage	0.82707 V
Current Density	0.19582 A/cm ²

For the impedance analysis, the equivalent circuit schematized in Figure 2 is considered with Frequency Range (200 mV) corresponding to 18131-4,8 Hz.

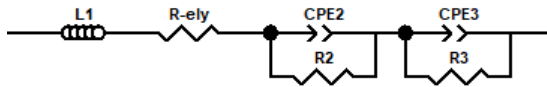


Figure 2: Scheme of the designed equivalent circuit.

The impedance and polarization resistance are respectively provided by eq. (4) and (5).

$$Z = i\omega L1 + R_{ely} + \left(\frac{1}{\frac{1}{R2} + \frac{1}{(Q2(i\omega)^{n2})}} \right) + \left(\frac{1}{\frac{1}{R3} + \frac{1}{(Q3(i\omega)^{n3})}} \right) \quad (4) \quad R_{pol} = R2 + R3 \quad (5)$$

$$\text{being the relationship between the actual voltage and polarization resistance: } \frac{\partial V}{\partial i} = R_{pol} \quad (6)$$

$$\text{The cell total efficiency is given by: } \varepsilon_{tot} = \varepsilon_{therm} + \varepsilon_{voltage} + \varepsilon_{fuel} \quad (7)$$

where:

$$\varepsilon_{therm} = \text{thermodynamic efficiency} = \frac{\Delta \hat{g}}{\Delta \hat{h}_{HHV}}$$

$$\Delta \hat{h}_{HHV} = \text{Higher heating value (kJ/mol)}$$

$$\Delta \hat{g} = \text{Gibbs free energy (kJ/mol)} = -nFE$$

$$n = \text{Number of electrons participating in the reaction (e}^{-}\text{eq)}$$

F = Faraday constant (C/e⁻eq)

$$E = \text{Nernst Voltage (V)} = E_0 - \frac{RT}{nF} \ln \left(\frac{1}{D_{H_2} P_{O_2}^{1/2}} \right)$$

$\epsilon_{\text{voltage}}$ = voltage efficiency = $\frac{V}{E}$

$$V = \text{actual voltage} = E_0 - \eta_{\text{therm}} - \eta_{\text{act,H2}} - \eta_{\text{act,O2}} - \eta_{\text{ohm}} - \eta_{\text{conc}}$$

$\eta_{\text{(act,H2)}}$ = Activation overvoltage, fuel electrode (V)

$\eta_{\text{(act,O2)}}$ = Activation overvoltage, air electrode (V)

η_{ohm} = Ohmic overvoltage (V)

η_{conc} = Concentration overvoltage (V)

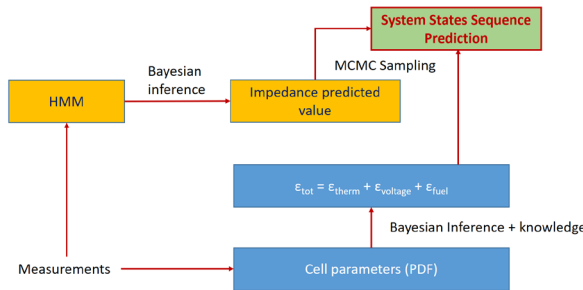
$$\epsilon_{\text{fuel}} = \text{fuel efficiency} = \frac{j/nF}{v}$$

j = Current density in the working point (A/cm²)

v = Hydrogen molar flow rate (mol/s)

2.6 Modeling framework

The model target values are the cell efficiency and the system impedance. The system variables are then represented as first level nodes in a Hierarchical Bayesian Net (HBN), representing an extension of Bayesian Networks to deal with structured domains. The approach uses the knowledge about the structure of the data to introduce a bias that can contribute to improving inference and learning methods. The nodes in an HBN are aggregations of simpler nodes. The impedance can provide an important insight into the system states transition, so that it is considered as emission in the Hidden Markov Model (HMM). The prediction of the system states sequence is the last level of the HBN, which provides the total cell efficiency. The overall modelling architecture is represented in Figure 3.



3. Results

Impedance values prediction

The parameters that determine the instantaneous impedance value are inserted in a Bayesian system, therefore their value is obtained from MCMC samplings in their probability distribution. The sampled values of the most relevant parameters are shown in Figure 4. From the simulation, it is possible obtaining the posterior predictive distribution for the cell impedance, as depicted in Figure 5. The posterior predictive distribution is continuously updated so that the impedance posterior predictive distribution represents the precursor for the internal leakage scenario, thus allowing a sort of dynamic hazard identification and hazardous initiating events detection.

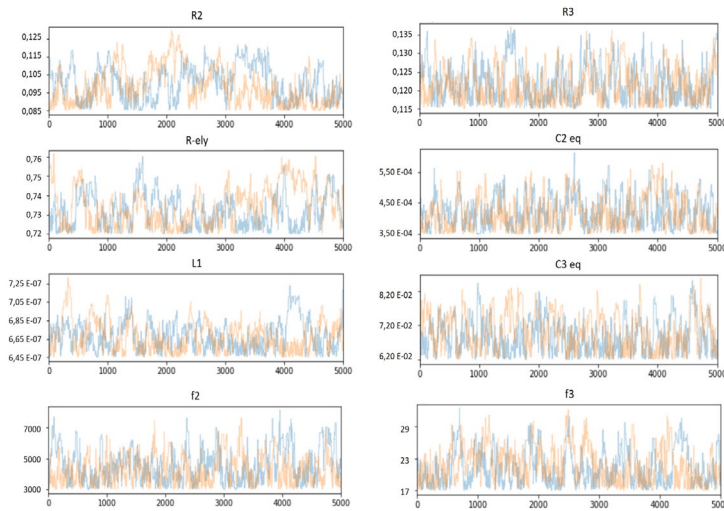


Figure 4: MCMC traces of the cell impedance parameters identified in the equivalent circuit reproduced in Figure 2.

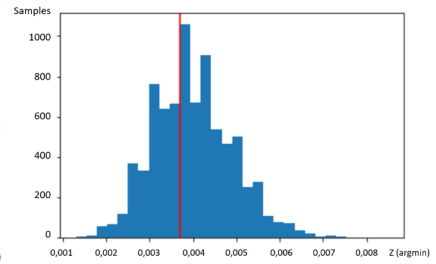


Figure 5: Impedance posterior predictive distribution.

4. Conclusions

As recently commented (Pasman et al., 2021), fully integration of sensors with machine learning and artificial intelligence-based method can make hidden abnormal features fully detectable with continuous updating for risk management purposes. The detection of gas leakages represents a relevant safety parameter, which can be predicted on time during the operations thus allowing an early detection of a potential accident scenario. This study introduces the impedance analysis as a reliable and effective tool to detect hydrogen leaks and oxygen concentrations in a single cell. As hydrogen leak rates increase, the impedance traces changed mostly within the mass transport region. The presented approach relies on a hybrid model incorporating different data driven models, HMM and HBN to provide updated and refined information. The model can infer the system states sequence and explores the interdependencies among the system components and their modification alongside process variables fluctuation. The preliminary experimental validation evidenced the model capability for predicting the impedance expected value with a good accuracy. Further experimental tests are under development to connect the cell efficiency with the predictive system and identify appropriate thresholds for early warning signals. Accordingly, potential hazardous deviations can be sorted from the early warnings gathered and a cause-consequence chain consistent with a conceptual bow-tie diagram may be developed, including all technical, operational and organisational safety barriers.

Acknowledgment

This research was partially funded by INAIL within the framework of the call BRIC/2019/ID2 (Project DYN-RISK).

References

- Galagedarage D.M., Khan F., 2019, Process fault prognosis using Hidden Markov Model–Bayesian Networks hybrid model, *Industrial & Engineering Chemistry Research*, 58, 12041–12053.
- Jia C., Han M., Chen M., 2017, Analysis of Gas Leakage and Current Loss of Solid Oxide Fuel Cells by Screen Printing, *E C S Transactions*, 78(1), 1533-1540.
- Lasia A., 2014, *Electrochemical Impedance Spectroscopy and its Applications*, Springer, New York .
- Mousa G., Golnaraghi F., DeVaal J., Young A., 2014. Detecting proton exchange membrane fuel cell hydrogen leak using electrochemical impedance spectroscopy method, *Journal of Power Sources*, 246, 110-116.
- Palazzi E., Perego P., Fabiano B., 2002, Mathematical modelling and optimization of hydrogen continuous production in a fixed bed bioreactor, *Chemical Engineering Science*, 57, 3819-3830.
- Palazzi E., Currò F., Fabiano B., 2020, Low rate releases of hazardous light gases under semi-confined geometry: A consequence based approach and case-study application, *Journal of Loss Prevention in the Process Industries*, 63, 104038. doi: 10.1016/j.jlp.2019.104038
- Pasman H.J., Fabiano B., 2021, The Delft 1974 and 2019 European Loss Prevention Symposia: Highlights and an impression of process safety evolutionary changes from the 1st to the 16th LPS. *Process Safety and Environmental Protection* 147, 80-91.
- Rasmussen, J.F.B., Hendriksen, P.V., Hagen, A., 2008, Study of Internal and External Leaks in Tests of Anode-Supported SOFCs, *Fuel Cells*, 8 (6), 385-393.
- Sato T., Kameya Y., 2001, Parameter learning of logic programs for symbolic-statistical, Modeling, *Journal of Artificial Intelligence Research*, 15, 391-454.
- Thagard P., Shelley C., 1997, Abductive reasoning: Logic, visual thinking, and coherence, Chapter In: Della Chiara M. L., Doets K., Mundici D., van Benthem J., (Eds), *Logic and Scientific Methods*, Synthese Library (Studies in Epistemology, Logic, Methodology, and Philosophy of Science), Vol 259, Springer, Dordrecht, Netherlands, 413-427.
- Tronstad T., Høgmoen Åstrand H., Haugom G.P., Langfeldt L., 2016, DNV-GL - EMSA Study on the use of Fuel Cells in Shipping, DNV GL – Maritime, available at <http://www.emsa.europa.eu>.
- Vairo T., Gualeni P., Reverberi A.P., Fabiano B., 2021, Resilience dynamic assessment based on precursor events: application to ship LNG bunkering operations, *Sustainability*, 13, 12, 6836.
- Van Biert L., Godjevac M., Visser K., Aravind P.V., 2016, A review of fuel cell systems for maritime applications, *Journal of Power Sources*, 327, 345-364.
- Vianello C., Bassani A., Mocellin P., Manenti F., Pirola C., Fabiano B., Colombo S., Maschio G., 2022, Hybrid risk-based LCA to improve the Acid Gas to Syngas (AG2S™) process, *Journal of Loss Prevention in the Process Industries*, 104694